

EMAS Core Material Modeling with LS-DYNA[®]

Yijian (Jack) Shi

*Engineered Arresting Systems Corporation
2239 High Hill Road, Logan TWP, NJ, 08085*

Abstract

With Lagrangian meshes and the LS-DYNA FEA explicit solver, Mat #63 – Crushable Foam is used to simulate the Phenolic foam – a candidate material for an EMAS core [7]. The simulated conditions include three scenarios: unconfined uniaxial compression, confined uniaxial compression and plate penetration into a large block. The three scenarios are purposely chosen for utilizing test data and validating simulation results. The simulations reveal that when an hourglass control is needed, the parameters for the control can significantly affect the results. The simulations with element formulations ELFORM=2 and 3 deliver better results than ELFORM=1. However, ELFORM=1 is the least expensive due to savings in computation time. ELFORM=3 is much more expensive than ELFORM=2 even with similar accuracy. When there is a symmetrical modeling condition, a reduced model size not only can save computational cost, but also sometimes can achieve greater accuracy. The simulation results are very sensitive to the value of TSC. For the very weak crushable material, a proper small value of TSC is preferred, instead of absolute zero.

At extreme large deformation, the Lagrangian meshes may not work well because of extreme element distortion, which is observed in the scenario of plate penetration into a large block.

Introduction

There were 44 overruns [1] worldwide in 2005. According to statistical data [3], “on average, 10 overruns annually occur in the United States”. These overruns often result in catastrophic property damages and serious injuries or fatalities. To minimize the casualties and property damages, EMAS (Engineered Material Arresting System) was developed [2] in 1990’s.

Since the debut of the EMAS system, it is accepted by aviation communities as an effective means to safely stop an aircraft in an overrun situation. The system is installed in a Runway Safety Area beyond a runway end. When an aircraft overruns into EMAS, the system generates resistive loads on the aircraft landing gears, which results in a gradual deceleration of the aircraft. The EMAS systems have successfully captured a number of aircraft overruns [3-5]. The results are in both saving lives and preventing aircraft damage.

There are about 50 EMAS systems [6] installed internationally up to date. The core materials used by EMAS systems are crushable materials, which are the major contributors to absorb aircraft kinetic energy. One type of candidate materials for the EMAS core, studied in Ref. [7], is crushable foam such as Phenolic foam. Detail modeling on the Phenolic foam with LS-DYNA is studied in this paper.

Material Modeling Consideration

The crushable foam which is often used for absorbing kinetic energy has lots of collapsible pore microstructures inside. Sometimes the pore structure is also called the cellular structure. The material behaviors under elastic-plastic large deformation conditions have been studied in a number of published papers [7-10]. Under a uniaxial compression test, the type of the crushable foam usually has the similar pattern on a stress-strain curve. As example, a compression test result of stress-strain curve for Phenolic foam [7] is shown in Fig. 1, in which the typical three characteristic deformation stages can be clearly observed.

In the early deformation stage and before the stress reaches a plastic plateau, the material is mainly deformed in a linear elastic manner and the deformation is very small. Near and before reaching the plateau, the material may experience a certain level of nonlinear deformation due to yielding of pore microstructure walls. In addition, at the beginning of the plateau, insignificant material softening can be observed, which may not be seen for some types of crushable foam, or even on opposite way - a certain level of hardening. The behaviors presented here are very much common on solid materials.

From about 5% to 70% deformation – within a fairly large range, the stress forms a relative constant plateau, which reflects that pore microstructures inside the material are consistently collapsed and generate consistent resistance. And the material is under irreversible progressive plastic failure, which can significantly absorb and dissipate energy. This stage makes up the main reason that the material is so popularly used for impact energy absorption and shock mitigation, which usually doesn't exist in other solid materials.

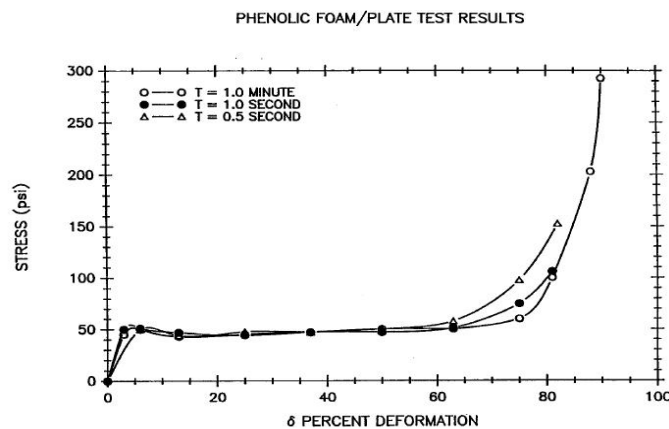


Fig. 1 An unconfined uniaxial compression test result [7]

At the last stage when the deformation reaches higher than 70%, all cellular pore microstructures are destroyed and the crushed material is under compaction. Therefore, the stress rapidly increases as the compression progresses further and the failed material quickly reaches up to an incompressible solid phase.

To maximize the EMAS energy absorption capability, properly modeling the crushable foam material and understanding its energy absorption process are extremely important. With some experimental data available [7], Material #63 – crushable-foam in LS-DYNA is selected to model this type of the crushable foam material. The validation of using Material #63 and normality of its parameters are investigated. Based on the availability of experimental data, three different simulation scenarios are considered. Material performances under a standard uniaxial compression on an unconfined cylindrical sample, a uniaxial compression on a confined cylindrical sample, and a penetration with a circular flat plate onto a large block are investigated, respectively. Simulations on uniaxial compression and plate penetration are compared with the experimental results.

To better understand simulation results, the effects of different conditions such as hourglass parameters, element formulations, model symmetric conditions and tensile stress cutoff (TSC) are discussed. Due to extremely low density of the Phenolic foam, the dynamic impact load in simulations is not given a special attention in this study.

Unconfined Uniaxial Compression Simulation

According to the test results shown in Fig. 1, a material uniaxial compression curve with similar stress-strain relationship in Fig. 2 is prepared for the computer simulation.

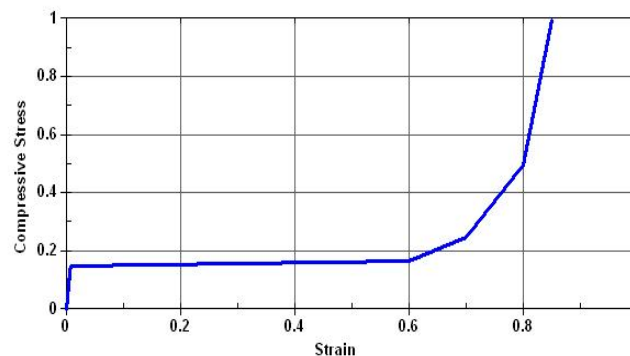


Fig. 2 Material uniaxial compression stress-strain used in simulation

The Lagrangian FEM with LS-DYNA is selected. Because the material is very brittle and has ignorable lateral deformation under compression, the Poisson ratio is very small. Therefore, the engineering uniaxial compression stress-strain curve can be considered as a uniaxial compression stress versus a volumetric strain.

For the uniaxial compression simulation, the 3-D mesh model is generated, which includes a top rigid plate and a Phenolic foam cylinder, as shown in Fig. 3. The Phenolic foam is modeled by Mat #63, and has the size: 50 mm in height and 25.4 mm in radius. A round top rigid plate compresses the Phenolic cylinder at the speed of 133 mm/sec. Because the modeling condition is axisymmetric, only a quarter of the full model is used.

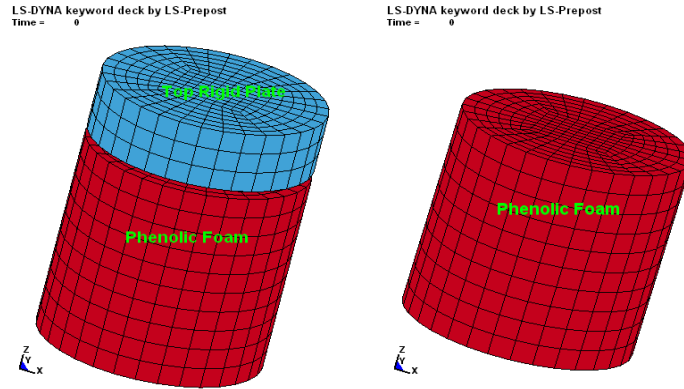


Fig. 3 3-D mesh model for the unconfined uniaxial compression simulation

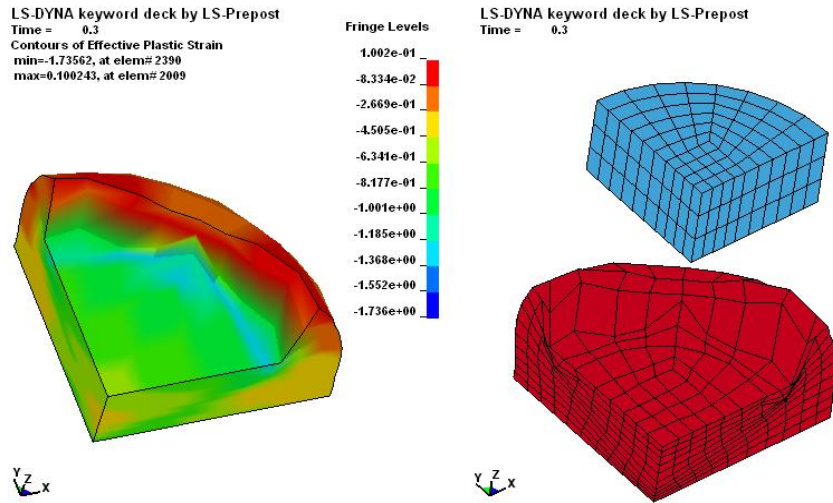


Fig. 4 Simulation results at t=0.3 sec for the unconfined uniaxial compression

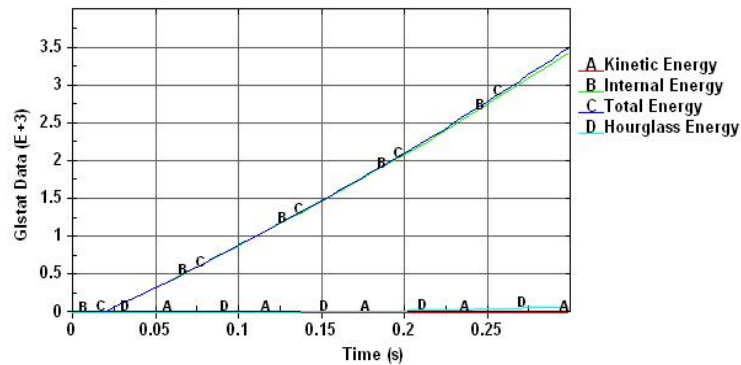


Fig. 5 Energy results for the unconfined uniaxial compression

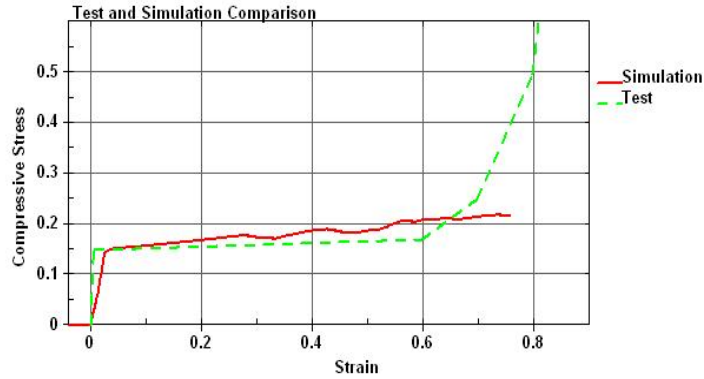


Fig. 6 Comparison between test and simulation for the unconfined uniaxial compression

With ELFORM=1 and default settings in CONTROL_HOURLGLASS, the simulation results are presented in Figs. 4 – 6. Because the top plate is not big enough, the Phenolic material is leaking out around the plate edge as the compression progresses. And since some of the material is no longer underneath the top plate (Fig. 4), lower resistance against the top plate may take place. The hourglass energy, as shown in Fig. 5, is very small, which means it needs a control and the current hourglass control does work well. The simulated average stress acting on the top plate (Fig. 6) is in good agreement with test data.

To further study the interaction between the plate and the Phenolic material, more simulations with different conditions from the previous base case are considered in following cases.

Case 1: Using Element Formulation ELFORM=3

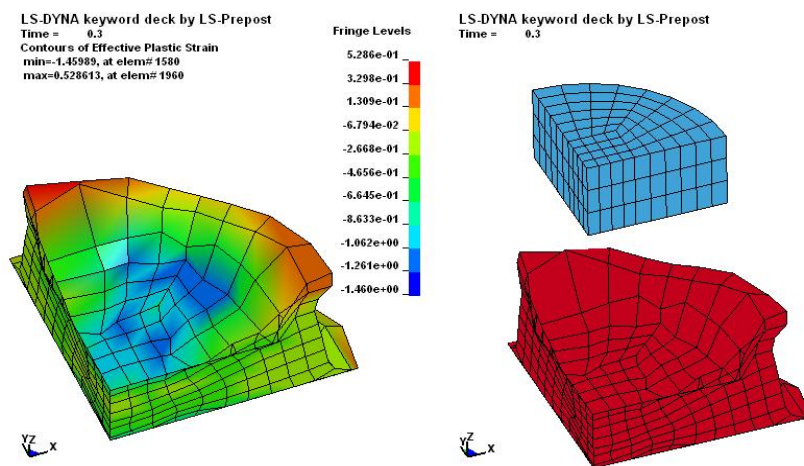


Fig. 7 Simulation results at t=0.3 sec for Case 1

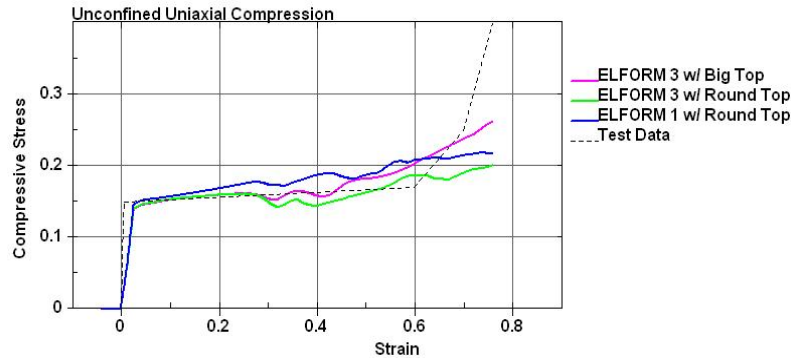


Fig. 8 Average stress for the unconfined uniaxial compression

In this case, all conditions are the same as in the base case, except ELFORM is 3 rather than 1. Figs. 7 and 8 show simulation results for Case 1. The similar material leaking (Fig. 7) can be observed. Compared to the average stress in the base case (Fig. 8), the stress in Case 1 with ELFORM=3 shows an agreement in a low strain range and a difference in a high strain range. In overall, ELFORM=3 gives a better match to test data than ELFORM=1. ELFORM=1 is slightly stiffer than ELFORM=3. However, ELFORM=1 uses the least computation time.

Case 2: Using Bigger Top Plate

To prevent material leaking as observed in both the base case and Case 1, this case uses a much bigger top plate. And all other conditions are the same as used in Case 1. The simulation results are presented in Figs. 8 and 9. In comparison to in Case 1, it's obvious that the average stress in Case 2 (Fig. 8) does increase at a high strain range due to no material leaking (Fig. 9).

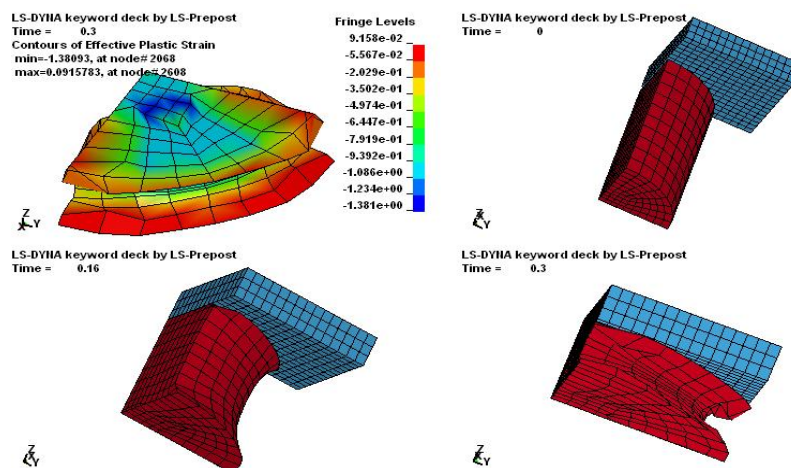


Fig. 9 Simulation results for Case 2

Case 3: Confining Bottom of the Phenolic Foam Cylinder

Based on the conditions in the base case (ELFORM=1, IHQ=1, QH=0.1), the physics with an additional confinement/constraint on the bottom of the Phenolic cylinder is simulated. The

simulation results for Case 3 are shown in Figs. 10 – 12. The bottom constraint can be observed from 3-D views in Fig. 10, when the deformation is significant large. The hourglass energy as shown in Fig. 11 is well controlled. In comparison to the base case, it’s interesting that the stress for Case 3 is the same, as shown in Fig. 12.

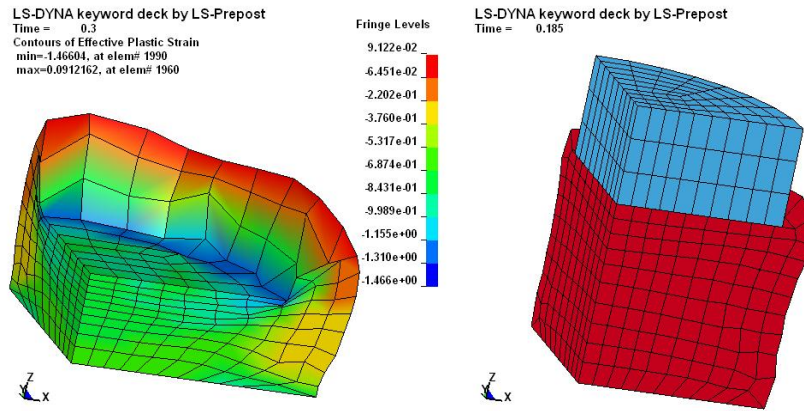


Fig. 10 Simulation results with confined bottom for Case 3

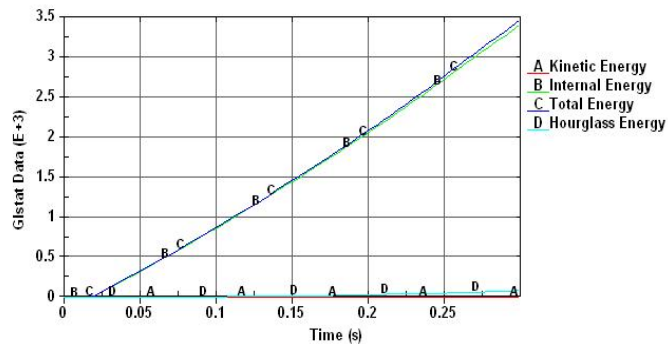


Fig. 11 Energy results with confined bottom for Case 3

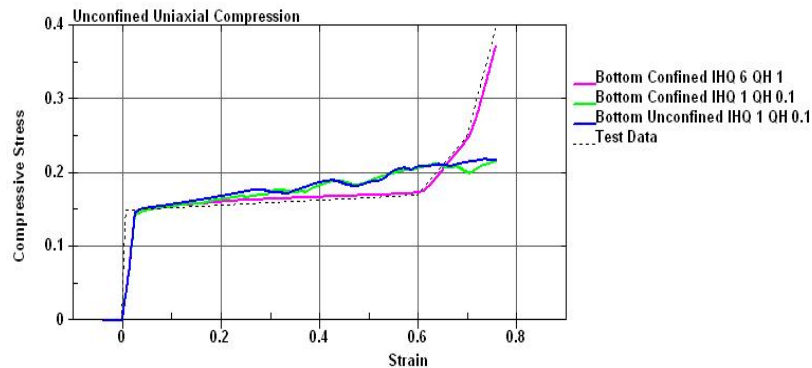


Fig. 12 Average stress for different hourglass controls and bottom confinement

Case 4: Using Different Hourglass Control

Based on the simulation conditions in Case 3 (IHQ=1 and QH=0.1), the new simulation case - Case 4 is constructed by changing the hourglass control parameters to IHQ=6 and QH=1. It's very interesting that the simulation results (Figs. 12 – 14) for Case 4 are completely different from what are obtained in Case 3. The 3-D views in Fig. 13 shows that the Phenolic cylinder is deformed only in the unaxial direction, which obviously doesn't make any sense. The hourglass control with IHQ=6 and QH=1 for Case 4 extremely overwhelms the compression reality. Of course the hourglass is definitely under control (Fig. 14). The simulated compression is similar to a confined volumetric compression, and the average stress for Case 4 closely matches the test data (Fig. 12).

To further confirm that the unrealistic compression is caused by the improper hourglass control and not caused by the condition of the bottom confinement on the Phenolic cylinder, an additional simulation without confining the bottom is performed. The result is shown in Fig. 15, and the unrealistic compression shows up again.

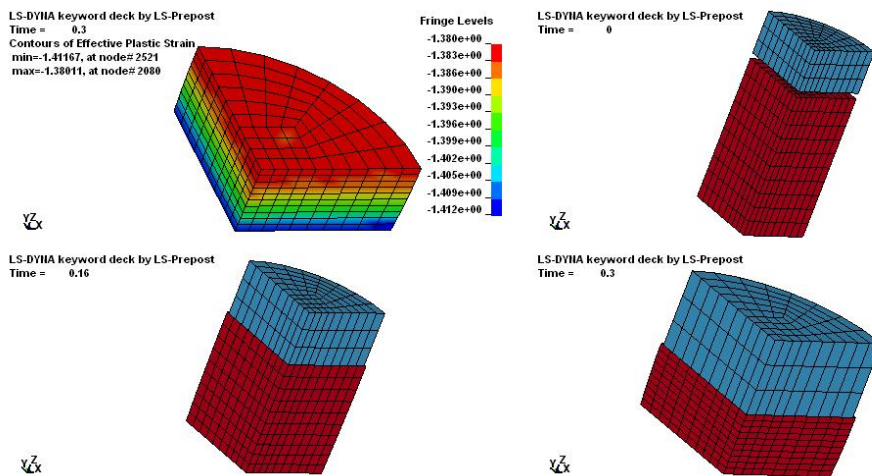


Fig. 13 Simulation results with IHQ=6, QH=1 for Case 4

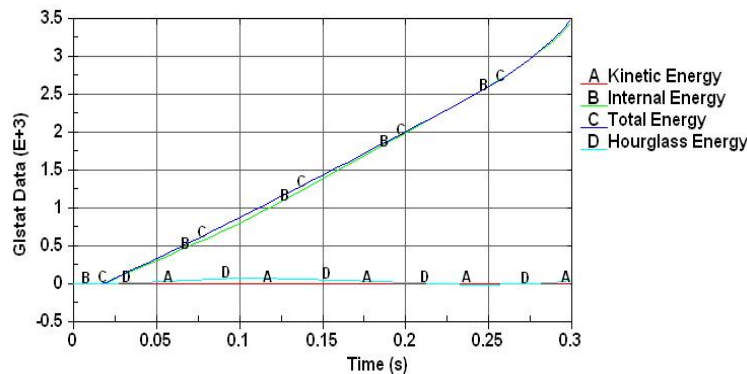


Fig. 14 Energy results with IHQ=6, QH=1 for Case 4

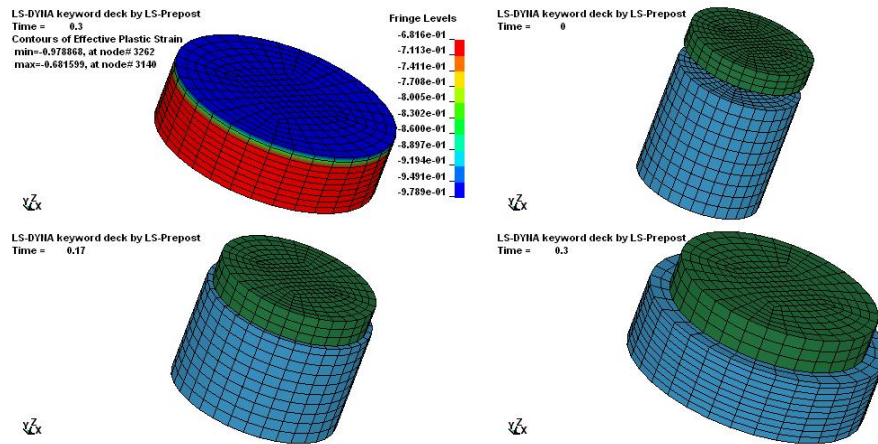


Fig. 15 Simulation results with IHQ=6, QH=1 and free bottom

Case 5: Using a Full Model with ELFORM=2 and 3

In all previous cases, only a quarter of the full model is simulated. To investigate whether there are any differences on simulation results between the quarter and full models, the full model is used in this case. Because the full model is axisymmetric, the simulation results for both the partial and full model theoretically should be the same.

However, from the simulation results (Figs. 16 - 18) with the full model for ELFORM=2 and 3, expected axisymmetric deformation in 3-D views cannot be observed, as shown in Figs. 16 and 18. This indicates that random numerical errors can be accumulated during computation and eventually large enough to affect final simulation results.

In addition, the average stresses for ELFORM=2 and 3 are very much similar (Fig. 17). However, the stresses for both full models show slightly stiffer than for the quarter model.

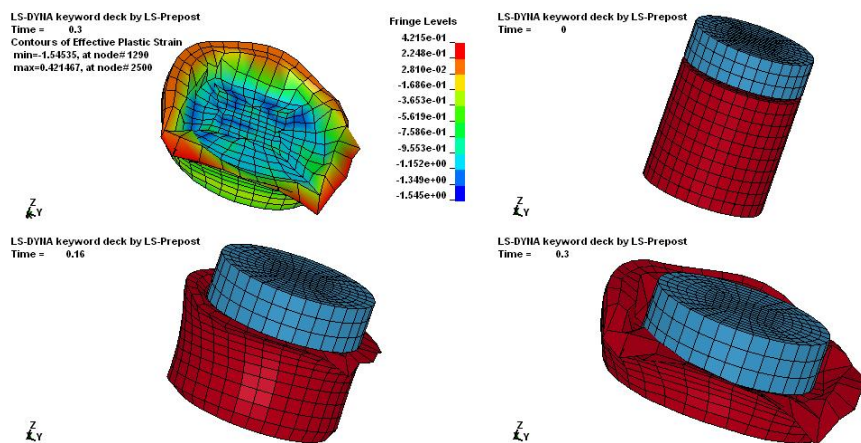


Fig. 16 Simulation results with ELFORM=3 for Case 5

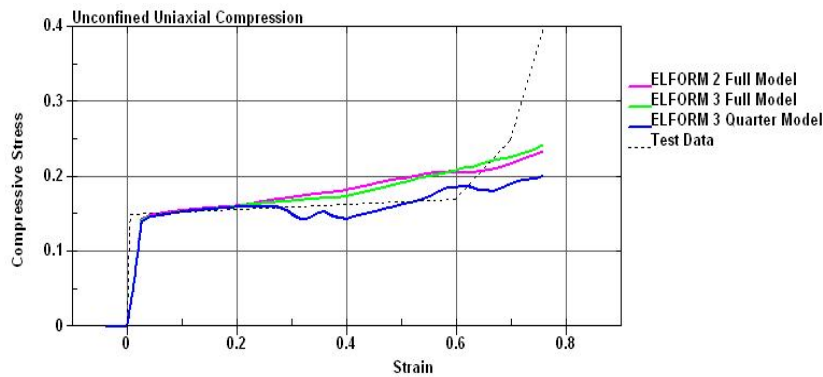


Fig. 17 Average stress comparison for the quarter and full models

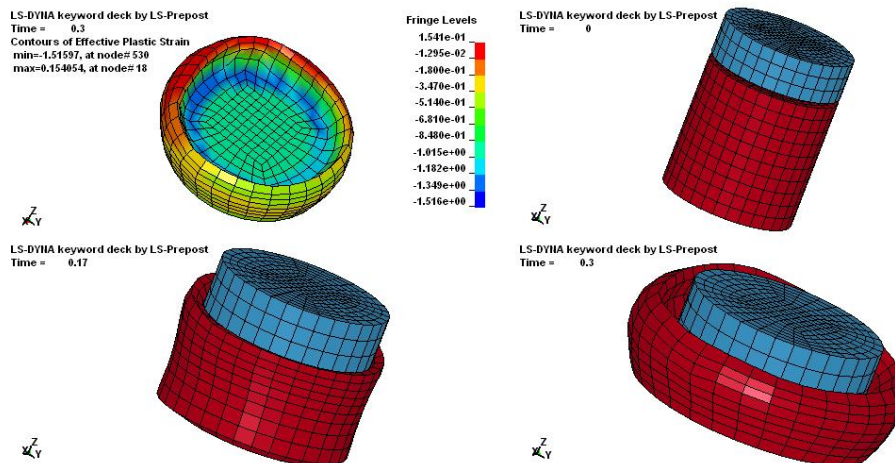


Fig. 18 Simulation results with ELFORM=2 for Case 5

For all discussions in above cases, preliminary conclusions on simulating unconfined Phenolic foam can summarize as:

1. When a hourglass control is needed, be careful with parameter values.
2. ELFORM=2 and 3 are better than ELFORM=1 in simulation accuracy. However, ELFORM=1 is the least expensive.
3. Utilizing symmetrical conditions to reduce a model size not only can save computing cost, but also can achieve greater accuracy.

Confined Uniaxial Compression Simulation

For the confined uniaxial compression simulation, conditions are the same as these used in the base case in the previous section. The only difference is that the Phenolic cylinder is confined inside a rigid cup.

The full model simulation results are presented in Figs. 19 – 21. In comparison to the result (Fig. 20) with ELFORM=3, compressed layers of the Phenolic foam with ELFORM=2 don't penetrate (Fig. 19) to each other, which of course indicates that ELFORM=2 is better. The average stress with ELFORM=2, shown in Fig. 21, is much smoother and in better agreement with test results than ELFORM=3, too. For ELFORM=1, the result is the same as for ELFORM=2, which is very much similar to a triaxial volumetric compression.

In addition, a quarter of the full model with ELFORM=3 is simulated (Fig. 22) for comparison purpose. It's not clear why the average stress for the quarter model, shown in Fig. 22, is more fluctuated and seems instable. With current simulation conditions, the results for the full and quarter models are slightly different.

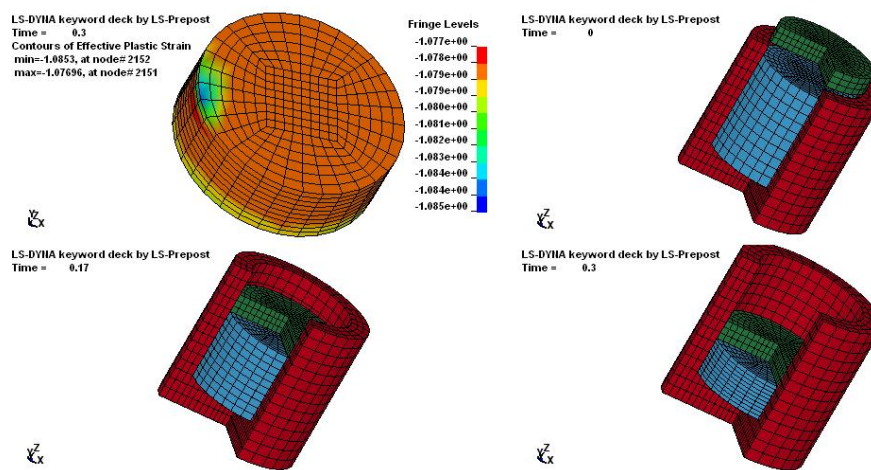


Fig. 19 Simulation results with ELFORM=2 for confined compression

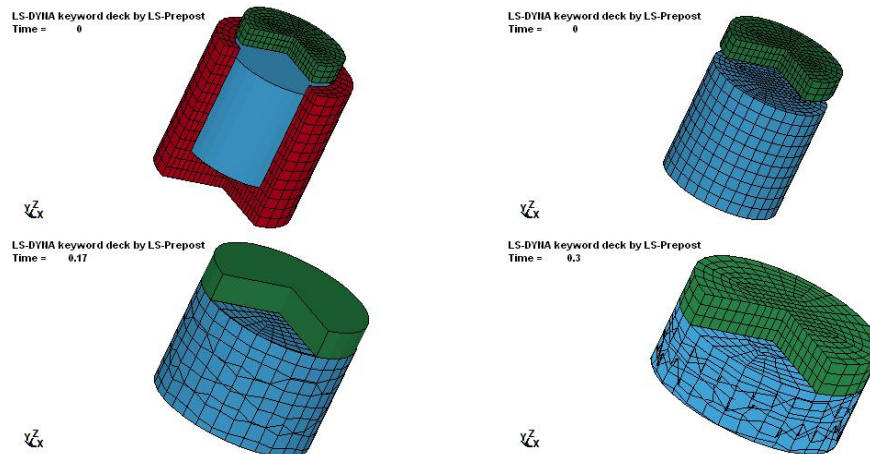


Fig. 20 Simulation results with ELFORM=3 for confined compression

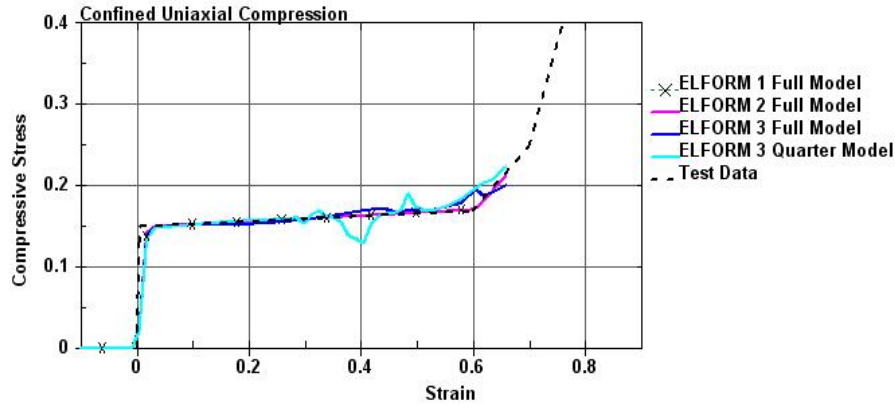


Fig. 21 Average stress on the top plate for the confined uniaxial compression

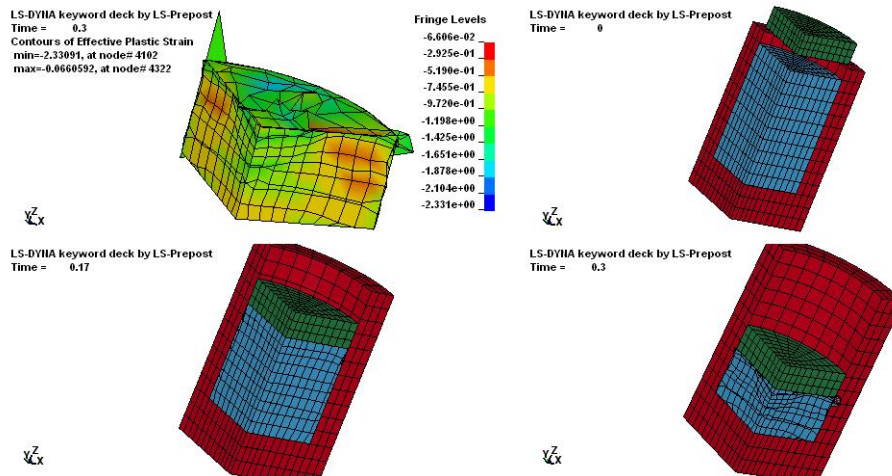


Fig. 22 Simulation results for a quarter model with ELFORM=3

For these four simulation cases, CPU usage is summarized in Table 1. According to the table, ELFORM=1 is the most inexpensive among these cases, because it can save computation time. ELFORM=3 is much more expensive than ELFORM=2, even with similar accuracy which has been discussed previously. Therefore, ELFORM=2 is recommended if computational cost is not a big concern. When there is a symmetrical modeling condition, a reduced model size (a quarter or half of a full model) can definitely save computational cost.

Table 1 CPU usage comparison

Simulation Case	# of Processors	CUP Time (s)
ELFORM=1 Full Model	4	1768
ELFORM=2 Full Model	2	10944
ELFORM=3 Full Model	4	12893
ELFORM=3 Quarter Model	4	5113

Plate Penetration Simulation

The scenario that a rigid plate at the speed of 25.4 mm/s penetrates into a large Phenolic block is simulated. To model the large Phenolic block, a size of 400 mm in diameter by 300 mm in height is used. The Phenolic material is modeled by Mat #63, which is the same as used in previous sections.

The simulation results with ELFORM =2, 3 and TSC=0.02 are presented in Figs. 23 – 25. The strain in Fig. 24 is defined as (penetration of the top plate)/(block height 300 mm), which is just for a reference purpose because the definition is obviously no longer accurate in theory. In comparison of Fig. 23 and 25, the material compression pattern underneath the plate for ELFORM=2 and 3 are very much similar. The similarity can also be observed on average stress in Fig. 24.

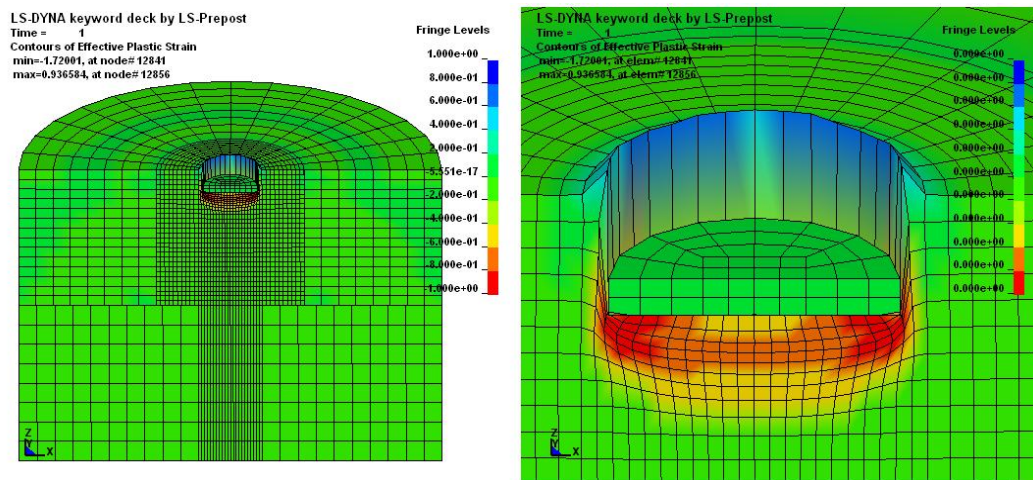


Fig. 23 Simulation results with ELFORM=2 for plate penetration

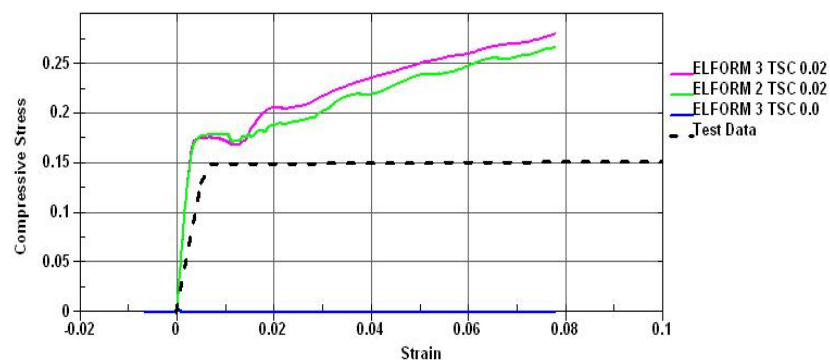


Fig. 24 Average stress on the top plate for plate penetration

It's very interesting that the deformed materials around and above the edges of the top plates are formed differently for ELFORM=2 and 3, and it's very difficult to judge which one is closer to

reality. For both cases, the large deformation around edges extremely distorts the Lagrangian meshes. Based on author's experience, the distortion often results in abnormal simulation termination due to critical computation errors. Solving the mesh distortion problem for extreme large deformation may demand other numerical methodologies such as SPH, ALE and FSI. Using these methodologies to improve the simulations is beyond the scope of this study.

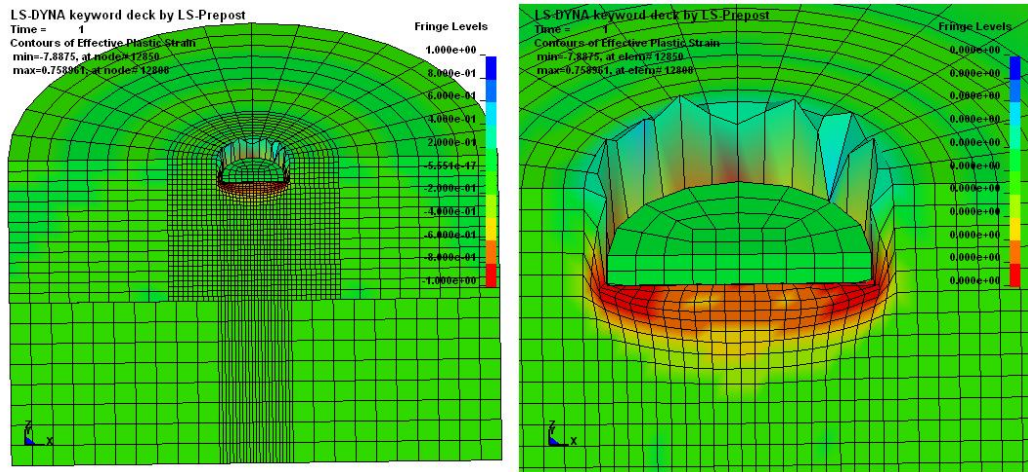


Fig. 25 Simulation results with ELFORM=3 for plate penetration

In addition, for the purpose of testing the simulation sensitivity on TSC, a case with TSC=0 and ELFORM=3 is simulated (see Figs. 26 and 27). It can be observed that the deformation of the Phenolic material turns more elastic accompanied with very little shear and compression (Fig. 26). The average stress for TSC=0 is extremely low (Fig. 27), which is almost invisible in Fig. 24.

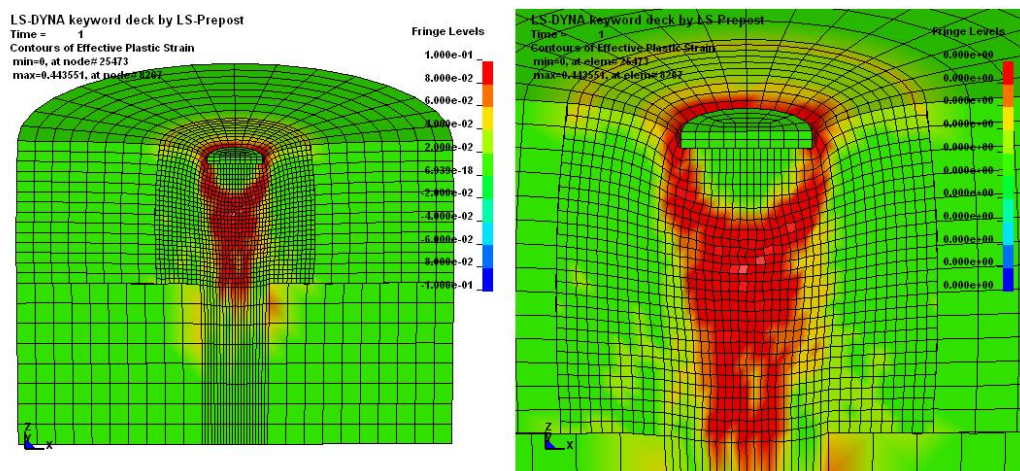


Fig. 26 Simulation results with ELFORM=3, TSC=0

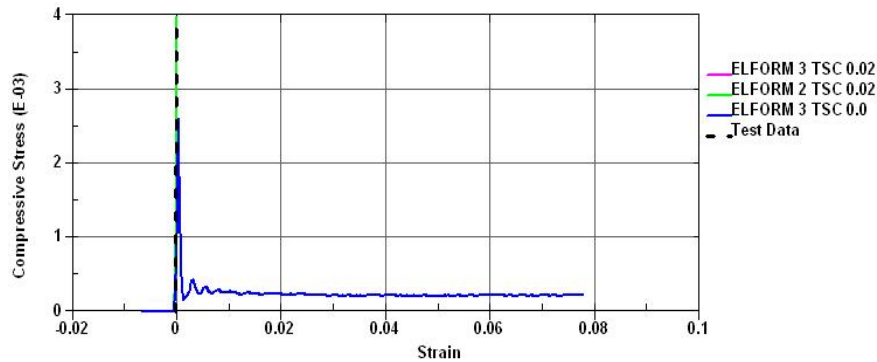


Fig. 27 A close-up view on average stress for plate penetration

Acknowledgments

This study was funded by Engineered Arresting Systems Corporation (ESCO-ZA). Thank ESCO-ZA for supporting the author to finish this paper. In addition, the author would like to give special thanks to Mr. Kevin Quan, Dr. Hong Zou, Mr. Tomas Giaquinto, Mr. Kent Thompson and Mr. Peter Mahal for reviewing this paper.

References

- [1] IFALPA, Living on a Prayer – 44 Runway Overruns in 2005, IFALPA Press Release, The Global Voice of Pilots, 06PRL016, 2006
- [2] Federal Aviation Administration, Engineered Materials Arresting Systems (EMAS) for Aircraft Overruns, Advisory Circular No: 150/5220-22A, 9/30/2005
- [3] Wayne Rosenkrans, Rethinking Overrun Protection, AVIATION SAFETY WORLD, Aug. 2006
- [4] John Croft, EMAS for the MASSES, Airport Magazine, Jan./Feb. 2004
- [5] David Heald, The EMAS Option, Airports International, Oct. 2005
- [6] Zodiac Aerospace, 50th EMAS Installation On-Track by End of 2009, Emergency Arresting Systems Division Braking News, Fall 2009
- [7] Robert F. Cook, Evaluation of Foam Arrestor Bed for Aircraft Safety Overrun Areas, Univ. of Dayton Research Institute, UDR-TR-88-07, Jan. 1988
- [8] J. G. Wang et al., A Microstructural Analysis for Crushable Deformation of Foam Materials, Comput. Mater. Sci. (2008)
- [9] V. Rizov, Elastic-Plastic Response of Structural Foams Subjected to Localized Static Loads, Materials and Design 27 (2006)
- [10] Qunli Liu and Brendan O'Toole, Behavior Pattern and Parametric Characterization for Low Density Crushable Foams, J. of Materials Processing Technology 191 (2007)

